Aberrant accumulation of EFEMP1 underlies drusen formation in Malattia Leventinese and age-related macular degeneration

Lihua Y. Marmorstein*†, Francis L. Munier‡, Yvan Arsenijevic‡, Daniel F. Schorderet‡, Precious J. McLaughlin*, Daniel Chung*, Elias Traboulsi*, and Alan D. Marmorstein*§

*Cole Eye Institute, and §Department of Cell Biology, Lerner Research Institute, Cleveland Clinic Foundation, 9500 Euclid Avenue, Cleveland, OH 44195; and ‡Unite d'Oculogénétique, Hôpital Ophtalmique Jules Gonin et Division de Génétique Médicale du CHUV, CH-1004 Lausanne, Switzerland

Communicated by C. Thomas Caskey, Cogene Biotech Ventures, Ltd., Houston, TX, August 15, 2002 (received for review July 2, 2002)

Malattia Leventinese (ML), an inherited macular degenerative disease, is closely reminiscent of age-related macular degeneration (AMD), the most common cause of incurable blindness. Both ML and AMD are characterized by extracellular deposits known as drusen between the retinal pigment epithelium (RPE) and Bruch's membrane. The mechanism underlying drusen formation is unknown. An Arg to Trp mutation in a gene of unknown function, *EFEMP1*, is responsible for ML, indicating EFEMP1 may be important in drusen formation. Here, we show that wild-type EFEMP1 is a secreted protein whereas mutant EFEMP1 is misfolded, secreted inefficiently, and retained within cells. In normal eyes, EFEMP1 is not present at the site of drusen formation. However, in ML eyes, EFEMP1 accumulates within the RPE cells and between the RPE and drusen, but does not appear to be a major component of drusen. Furthermore, in AMD eyes, EFEMP1 is found to accumulate beneath the RPE immediately overlaying drusen, but not in the region where there is no apparent retinal pathology observed. These data present evidence that misfolding and aberrant accumulation of EFEMP1 may cause drusen formation and cellular degeneration and play an important role in the etiology of both ML and AMD.

The macula, a central circular area of the retina 5 to 6 mm in diameter with the fovea at its center, facilitates central vision and high-resolution visual acuity. Various diseases causing macular degeneration result in severe and irreversible loss of vision. Malattia Leventinese (ML), also known as Doyne honeycomb retinal dystrophy, is a rare autosomal dominant macular degenerative disease with high penetrance (1–3). Onset of ML is generally in midlife but can vary from childhood until old age (4). An early characteristic feature of ML is the presence of amorphous sub-retinal pigment epithelium (RPE) deposits known as drusen between the RPE and Bruch's membrane (1, 5). At a later stage of the disease, ML exhibits a variety of clinical and histopathological features, including decreased visual acuity, geographic atrophy, pigmentary changes, and choroidal neovascularization (6). Drusen are also an early hallmark of age-related macular degeneration (AMD), a heterogeneous late onset macular degenerative condition (7). ML exhibits features more consistent with AMD than any other heritable macular disorder. Except for a late age of onset, AMD shares the typical clinical features of ML (8). AMD accounts for approximately 50% of registered blindness in the developed world (9, 10). More than 20% of the population over 65 years of age is affected with AMD. The molecular mechanism responsible for drusen formation and other retinal pathology observed in ML or AMD is currently unknown.

A single mutation, Arg-345 to Trp (R345W) in the gene *EFEMP1* (for epidermal growth factor-containing fibrillin-like extracellular matrix protein 1), was found to be responsible for ML (11). To date, no mutation in *EFEMP1* has been found to be associated with AMD (11). Initially described as S1-5 (12), also known as FBNL (13) or fibulin-3 (14), *EFEMP1* is a widely expressed gene of unknown function. The human *EFEMP1* cDNA encodes a putative protein of 493 aa, with a predicted molecular mass of 55 kDa (12). It is highly conserved among humans and rodents (12, 15). Based on its sequence similarity to the fibulin and fibrillin gene families, EFEMP1 is predicted to be an extracellular matrix protein, but is otherwise completely uncharacterized.

To investigate how the mutation in EFEMP1 causes ML and whether EFEMP1 plays a role in AMD, we generated monoclonal and polyclonal antibodies to characterize wild-type and mutant EFEMP1. Immunoanalysis and pulse–chase secretion assays in cell cultures and human donor tissues indicate that misfolding and abnormal accumulation of EFEMP1 is linked to drusen formation in both ML and AMD.

MEDICAL SCIENCES

Materials and Methods

Antibody Production. A mouse monoclonal antibody (Mab3-5) against EFEMP1 was made by using a GST-EFEMP1 fusion protein containing amino acids 107 to 493 of EFEMP1 as antigen. The *EFEMP1* cDNA was amplified by PCR from a human placenta cDNA library, subcloned into the pGEX-4T-2 vector, and verified by sequencing. The fusion protein was expressed in BL21 bacterial cells, and purified by affinity chromatography with glutathione Sepharose 4B. A rabbit polyclonal antibody (Pab) was generated against a synthetic peptide corresponding to residues 339 through 353 of the predicted human EFEMP1 amino acid sequence. This peptide was chosen based on its antigenicity and sequence specificity for EFEMP1 compared with the sequences in the public database, and because it contained the R345 residue mutated in ML.

Cell Culture. RPE-J cells were grown in DMEM containing 4% FBS at 32°C. All of the other cell lines were grown at 37°C. The 293 cells were maintained in DMEM containing 10% FBS, D407 cells in DMEM containing 3% FBS, and ARPE-19 cells in DMEM/F12 containing 10% FBS.

Expression of Recombinant Wild-Type and Mutant EFEMP1. The full-length human *EFEMP1* cDNA was amplified by PCR from a human placenta cDNA library, subcloned into a mammalian expression vector, pAdlox, and verified by sequencing. The mutation for R345W was generated by using the QuikChange site-directed mutagenesis method (Stratagene). To generate EFEMP1-RFP (red fluorescent protein) fusion protein, full-length *EFEMP1* cDNA was fused at the N terminus of *RFP* in pDsRed1-N1. The *EFEMP1-RFP* DNA fragment was then transferred into pAdlox. Plasmids were transfected into 293 or RPE-J

Abbreviations: ML, Malattia Leventinese; AMD, age-related macular degeneration; RPE, retinal pigment epithelium; EFEMP1, epidermal growth factor-containing fibrillin-like extracellular matrix protein 1; RFP, red fluorescent protein.

†To whom reprint requests should be addressed. E-mail: marmorl@ccf.org.

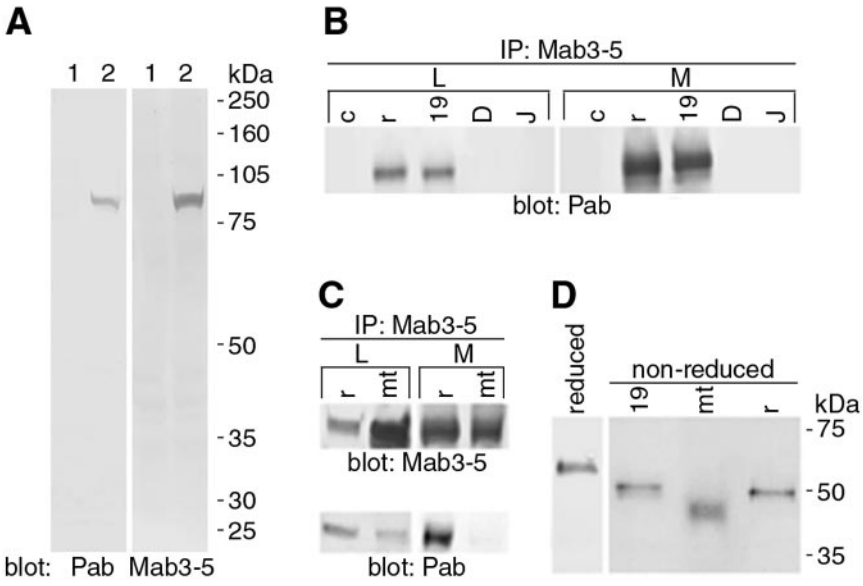

Fig. 1. Characterization of EFEMP1 antibodies and wild-type and mutant EFEMP1 protein. (*A*) Lysates of 293 cells transfected with control vector (lane 1) or *EFEMP1-RFP* DNA (lane 2) were immunoblotted with Pab or Mab3-5 antibody against EFEMP1. The only band detected in the blots corresponds to the EFEMP1-RFP fusion protein (84 kDa) in the *EFEMP1-RFP* transfected cell lysates, indicating the high specificity of these antibodies. (*B*), Cell lysates (L) and media (M) of 293 cells transfected with control vector (lane c) or *EFEMP1* cDNA (lane r), or untransfected ARPE-19 (lane 19), D407 (lane D), and RPE-J (lane J) cells were immunoprecipitated with Mab3-5 and blotted with Pab. A band with a relative molecular mass of ≈55 kDa was detected in both the lysates and media of 293 cells transfected with *EFEMP1* cDNA and ARPE-19 cells. (*C*) Lysates (L) and media (M) of 293 cells transfected with *EFEMP1* cDNA without (lane r) or with the R345W mutation (lane mt) were immunoprecipitated with Mab3-5 and blotted with Mab3-5 (*Upper*) or Pab (Lower). Note mutant EFEMP1 comigrates with wild-type EFEMP1. There is noticeably more mutant EFEMP1 in the lysates than the media compared with wild-type EFEMP1. Note Pab recognizes mutant EFEMP1 poorly. (*D*) Endogenous EFEMP1 in ARPE-19 medium (lane 19) and recombinant wild-type (lane r) and mutant (lane mt) EFEMP1 expressed in 293 transfectant media were analyzed under nonreducing conditions (non-reduced). A control of EFEMP1 under reducing conditions is shown (reduced). Note that mutant EFEMP1 migrates faster than the wild type in nonreducing conditions.

cells by using Lipofectamine (GIBCO). Forty-eight hours after transfection, cells were analyzed.

Immunoprecipitation and Immunoblotting. Immunoprecipitation and immunoblotting were performed as before (16). Briefly, cell lysates (500 μg of total protein) or conditioned media (1 ml) were immunoprecipitated with 10 μg of Mab3-5. Immunoprecipitates or cell lysates (50 μg) were separated on a 10% SDS/PAGE gel, transferred to a poly(vinylidene difluoride) membrane, and blotted with Mab3-5 or Pab at a dilution of 1:200. For nonreducing conditions, to avoid the interference of the IgG heavy chain in interpreting results, Mab3-5 was covalently coupled to protein A Sepharose as described (17) before it was used in immunoprecipitation. The immunoprecipitates were resuspended in sample buffer containing no β-mercaptoethanol.

Pulse–Chase Assay. Pulse–chase assay was performed as described (18). Briefly, RPE-J cells were transfected with human full-length *EFEMP1* cDNA without or with the R345W mutation. Forty-eight hours after transfection, cells were pulsed for 30 min with cysteine and methionine free medium containing 1 mCi/ml (1 Ci = 37 GBq) of [^{35}S]cysteine. Cells were then lysed (L) and media collected (M) after 0, 0.5, 1, 2, 4, 6, 8, and 24 h. EFEMP1 was immunoprecipitated with Mab3-5, and separated on 10% SDS/PAGE gel. The gel was fixed, dried, exposed to a storage phosphor screen, and analyzed by using a Typhoon PhosphorImager (Molecular Dynamics) and IMAGEQUANT 5.0 software.

Immunohistochemistry and Immunofluorescence Staining. Immunohistochemistry and immunofluorescence staining was performed as described (19). Briefly, human donor eyes were fixed in neutral buffered formalin after a small incision in the pars planar region (2–3 mm) with a no. 11 blade. Tissues were processed for paraffin sections. After deparaffinization, sections were subjected to pressurized heat-mediated antigen retrieval and stained with EFEMP1 or a control mouse monoclonal antibody RET-PE2 in equivalent dilutions. The control antibody recognizes a species-specific epitope in rat extracellular matrix metalloproteinase inducer (EMMPRIN). Diaminobenzidine (DAB; brownish color) or Vector VIP substrate (VIP; purple color, Vector Laboratories) was used as substrate. When DAB was used as substrate, nuclei were counterstained with nuclear fast red, and, when VIP was used as substrate, nuclei were not stained. RPE-J cells expressing wild-type or mutant EFEMP1 on coverslips were fixed in −20°C methanol and stained with Mab3-5 and a Texas red conjugated anti-mouse IgG secondary antibody. Nuclei were stained with 4′,6-diamidino-2-phenylindole (DAPI).

Results

Generation of Antibodies. To investigate how the mutation in EFEMP1 causes ML, a mouse monoclonal antibody (Mab3-5) against EFEMP1 was made by using a GST-EFEMP1 fusion protein as antigen. We also produced a rabbit polyclonal antibody (Pab) against a synthetic peptide corresponding to residues 339 through 353 of the predicted human EFEMP1 amino acid sequence. This peptide was chosen based on its antigenicity and sequence specificity for EFEMP1, compared with the sequences in the public database, and because it contained the arginine residue mutated in ML. Both Mab3-5 and Pab exhibit high specificity and titer (Fig. 1*A*). In ELISA, Mab3-5 does not recognize the peptide used as antigen for Pab (data not shown), indicating that Mab3-5 and Pab recognize different epitopes in EFEMP1 protein.

Both Wild-Type and Mutant EFEMP1 Are Secreted Proteins. To characterize EFEMP1 protein, human RPE-derived cell lines

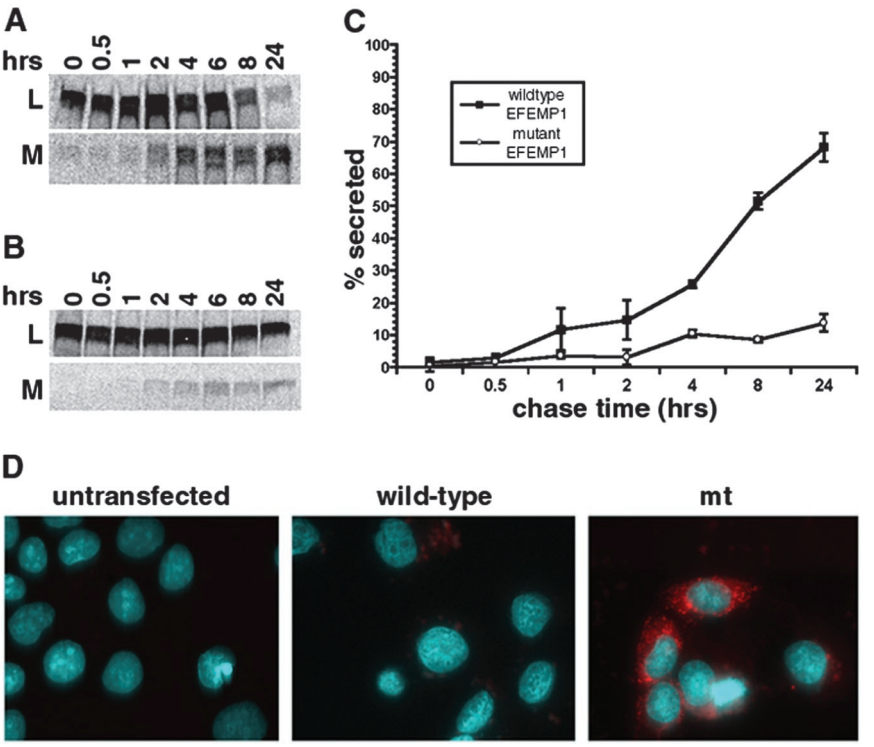

Fig. 2. Comparison of wild-type and mutant EFEMP1 secretion. Pulse–chase secretion assays were performed for EFEMP1 in RPE-J cells transfected with the full-length *EFEMP1* cDNA without (*A*) or with the R345W mutation (*B*). (*C*) The percentage of secretion in pulse–chase secretion assays was derived from the protein amount in the medium divided by the combining amount in the lysate and medium at each time point. By 24 h of chase, nearly 70% of the wild-type EFEMP1 was in the medium, whereas only 13% of mutant EFEMP1 was secreted. (*D*) Transfected RPE-J cells stained with monoclonal antibody 3-5 (red). The nuclei were stained with 4′,6-diamidino-2-phenylindole (DAPI; blue).

ARPE-19 and D407 and a rat RPE cell line RPE-J were analyzed by immunoprecipitation and immunoblotting with Mab3-5 and Pab. EFEMP1 was detected in ARPE-19 (Fig. 1*B*, lane 19), but not in D407 (Fig. 1*B*, lane D) or RPE-J (Fig. 1*B*, lane J). The endogenous EFEMP1 in ARPE-19 comigrated at ≈55 kDa, with the recombinant EFEMP1 protein expressed in 293 cells transfected with the full-length human *EFEMP1* cDNA (Fig. 1*B*, lane r). The 293 cells have no detectable endogenous EFEMP1 (Fig. 1*B*, lane c). EFEMP1 was detected in both cell lysates (Fig. 1*B*, L) and culture media (Fig. 1*B*, M), suggesting that EFEMP1 is a secreted protein, a finding further confirmed by pulse–chase analysis (Fig. 2).

To characterize the ML-associated R345W mutation, 293 cells were transfected with the full-length human *EFEMP1* cDNA with or without the R345W mutation and analyzed by immunoblotting with Mab3-5 (Fig. 1*C Upper*) or Pab (Fig. 1*C Lower*) after immunoprecipitation with Mab3-5. Mutant EFEMP1 (Fig. 1*C*, lane mt) comigrated with the wild-type protein (Fig. 1*C*, lane r) and was also detected in both cell lysate (Fig. 1*C*, L) and culture medium (Fig. 1*C*, M). However, the mutant EFEMP1 was noticeably more abundant in the lysate and less abundant in the medium than the wild type. Interestingly, antibody Pab, which was raised against the peptide containing the Arg-345 mutated to Trp, recognizes mutant EFEMP1 poorly (Fig. 1*C Lower*).

Mutant EFEMP1 Is Misfolded. To determine whether wild-type and mutant EFEMP1 exist in different forms, endogenous EFEMP1 in ARPE-19 medium, recombinant wild-type and mutant EFEMP1 expressed in 293 transfectant media were analyzed under nonreducing conditions (Fig. 1*D*, lanes 19, r, and mt). This analysis indicates that both wild-type and mutant EFEMP1 are monomeric. EFEMP1 proteins migrate slightly faster in nonreducing conditions than they do under reducing conditions, suggesting the existence of intramolecular disulfide bonds. Interestingly, under nonreducing conditions, mutant EFEMP1 migrates faster than the wild-type protein, indicating that the intramolecular disulfide bonds are different in the mutant compared to wild-type EFEMP1. Disulfide bonding is one of the most important stabilizing forces in the tertiary structure of secretory proteins (20). The R345W mutation does not involve a cysteine; thus, it is reasonable to conclude that mutant EFEMP1 is misfolded.

Mutant EFEMP1 Is Secreted Inefficiently and Retained Within Cells. To examine the effect of this change in conformation on secretion and to determine whether mutant EFEMP1 is indeed secreted less efficiently than wild-type EFEMP1, pulse–chase secretion assays were performed by using RPE-J cells transfected with human *EFEMP1* cDNA with or without the R345W mutation (16). Wild-type EFEMP1 was consistently detected in both cell lysates (Fig. 2*A*, L) and media (Fig. 2*A*, M). The secretion process is relatively slow, presumably due to the large number of disulfide bonds that must be correctly formed in the protein. EFEMP1 contains 40 cysteines, the most abundant amino acid in EFEMP1, accounting for 8% of the total amino acid content of the protein. The half time of secretion of EFEMP1 was determined to be 8 h. In contrast to wild-type EFEMP1, the vast majority of mutant EFEMP1 was consistently detected in cell lysates (Fig. 2*B*, L). Even after 24 h of chase, only 13% of mutant EFEMP1 was secreted into the medium in comparison to nearly 70% of wild-type EFEMP1 (Fig. 2*C*), an ≈5-fold difference.

To determine whether mutant EFEMP1 accumulates within the cells, immunofluorescence staining was performed with Mab3-5 on RPE-J cells expressing wild-type or mutant EFEMP1 (Fig. 2*D*, red color). Cells expressing wild-type EFEMP1 exhib-

ited little staining. When positive for EFEMP1, the staining was usually confined to a dim perinuclear pattern (Fig. 2*D*, wild-type). Cells expressing mutant EFEMP1, on the other hand, exhibited intense staining of numerous punctate regions throughout the cytoplasm suggestive of endoplasmic reticulum (Fig. 2*D*, mt). These data indicate that, in contrast to the wild-type protein, mutant EFEMP1 secretes inefficiently and accumulates within cells.

The Absence of EFEMP1 at the Site of Drusen Formation in Normal Eyes. To determine the distribution of EFEMP1 protein in retina, human donor eyes from seven individuals (aged 40, 55, 75, 75, 76, 84, and 91 yr) were analyzed by immunohistochemistry with Mab3-5 or Pab. EFEMP1 protein was found predominantly in the photoreceptor inner and outer segment region and the nerve fiber layer, but was also detectable in the outer nuclear layer, and inner and outer plexiform layers (Fig. 3*A* and Fig. 4*B*). Surprisingly, no signal was observed in the RPE, Bruch's membrane, the choroid, or small hard drusen (Fig. 4*B*, asterisk), indicating that EFEMP1 is not normally present at the site of drusen formation.

EFEMP1 Accumulates Between RPE and Drusen in both ML and AMD. To determine how the R345W mutation affects EFEMP1 localization *in vivo*, we analyzed a donor eye from an 86-yr-old female ML patient. The donor was determined to be homozygous for the R345W mutation in *EFEMP1* by mutation screening (11). The clinical course of the disease in this patient was indistinguishable from heterozygous individuals (21). Histological analysis reveals severe atrophy, absence of photoreceptor and RPE cells, and large fibrous scars in the macula of this eye (data not shown). In the peripheral retina, large continuous drusen and short outer segments were observed. Even the best preserved region of peripheral retina exhibited an abnormal "rosette" pattern of the photoreceptor outer segments, hyperplastic RPE, and thickening of Bruch's membrane (data not shown). In striking contrast to the absence of EFEMP1 in the sub-RPE region of normal human eyes, an intense line of EFEMP1 staining beneath the RPE overlaying drusen was observed in ML (Fig. 3 *C*, *E*, and *G*, arrowheads). EFEMP1 accumulation within some RPE cells was also observed (Fig. 3 *C* and *G*, asterisk). A few drusen were stained by the EFEMP1 antibody (Fig. 3*C*, white arrow) although the intensity of the staining was always lower than the region between the RPE and drusen. In some drusen, a defined region adjacent to the RPE appeared stained with the remainder of the deposits apparently devoid of EFEMP1 (Fig. 3*G*, black arrow). In summary, most drusen in the ML eye did not stain positive with the anti-EFEMP1 antibody (Fig. 3*E*), whereas the region between the RPE and the deposit always did. These data suggest that, whereas mutant EFEMP1 accumulates beneath and within RPE cells overlaying drusen, it may not be a major component of drusen associated with ML.

To determine the pattern of EFEMP1 distribution in AMD eyes, human donor eyes from seven different patients clinically diagnosed with AMD (aged 75, 77, 79, 85, 86, 87, and 89 yr old) were probed with Mab3-5 by immunohistochemistry. None of these AMD patients carried the R345W mutation in *EFEMP1* (data not shown). The pattern of EFEMP1 staining in otherwise normal appearing regions of the periphery in all of the AMD eyes examined (Fig. 4*E*) was identical to that observed in normal eyes (Fig. 4*B*). Again, the photoreceptor inner and outer segment region and the nerve fiber layer were found to be the primary regions of EFEMP1 distribution with no staining observed in the RPE, Bruch's membrane, or the choroid (Fig. 4*E*). Remarkably, in the macula of AMD eyes, we invariably observed heavy EFEMP1 staining beneath RPE cells overlaying soft drusen (Fig. 4 *H*, *I*, *K*, and *L*) and in basal deposits (Fig. 4 *N* and *O*). Although variable in intensity, EFEMP1 staining was typically less intense in soft drusen compared with the region between the drusen and the RPE. In some AMD eyes, heavier EFEMP1 staining along the apical surface of the RPE but less intense staining in the photoreceptor inner and outer segment region were observed (Fig. 4 *K*, *L*, *N*, and *O*). A similar pattern of staining was observed in soft drusen or basal deposits in the periphery of the eye. EFEMP1 staining was not observed to be associated with small hard drusen. From these data, we conclude that, similar to ML, EFEMP1 accumulates between the RPE and soft drusen and in basal deposits, but it does not appear to be a major component of drusen in AMD eyes.

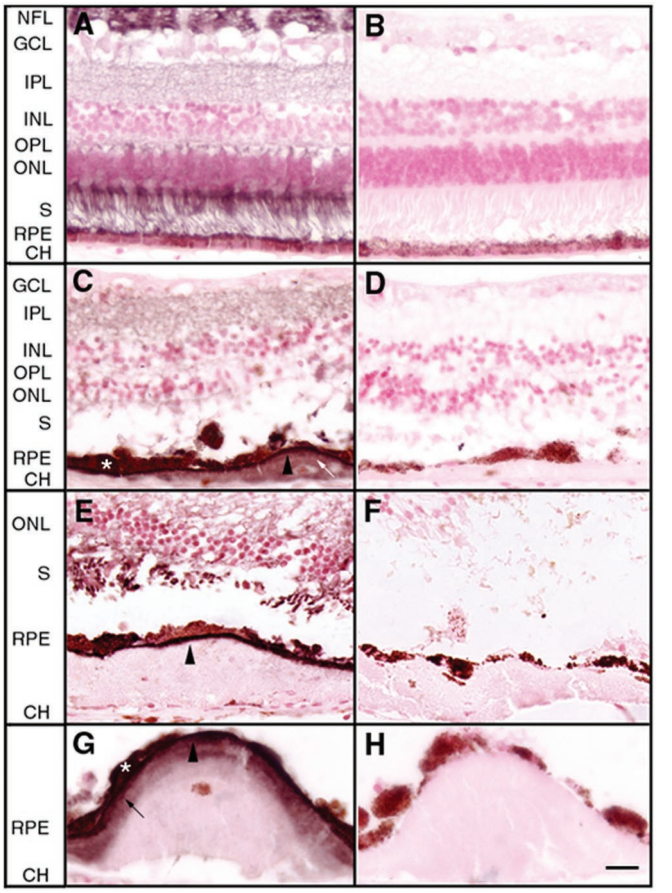

Fig. 3. The distribution of EFEMP1 in normal or ML eyes. Paraffin sections of human donor eyes were probed with Mab3-5 or a control mouse monoclonal antibody RET-PE2 in equivalent dilutions to Mab3-5. The control antibody recognizes a species-specific epitope in rat extracellular matrix metalloproteinase inducer (EMMPRIN). Diaminobenzidine (DAB; brownish color) was used as substrate, and nuclei were counterstained with nuclear fast red. (*A* and *B*) Normal eye from a 55-yr-old male (*A*) was stained with Mab3-5 and (*B*) the control antibody. Note that EFEMP1 staining is predominantly associated with the nerve fiber layer (NFL) and the photoreceptor inner and outer segments (S). Less intense staining was observed in the outer nuclear layer (ONL) and the inner (IPL) and outer (OPL) plexiform layers. No staining was observed in the RPE, Bruch's membrane, the choroid (CH), or the inner nuclear layer (INL). (*C–H*) Eye from an 86-yr-old female ML patient homozygous for the R345W mutation in *EFEMP1* gene. *C*, *E*, and *G* were stained with Mab3-5, and *D*, *F*, and *H* with the control antibody. An intense line of EFEMP1 staining separates the RPE from the drusen beneath (*C*, *E*, and *G*, arrowheads). Some RPE cells overlaying drusen were heavily stained by Mab3-5 (*C* and *G*, asterisk). A few drusen were stained by the EFEMP1 antibody (*C*, white arrow) although the intensity of the staining was always lower than the region between the RPE and drusen. In some drusen, a defined region adjacent to the RPE appeared stained, with the remainder of the deposits apparently devoid of EFEMP1 (*G*, black arrow). GCL, ganglion cell layer. [Scale bar = 40 μm (*A–F*) and 20 μm (*G* and *H*).]

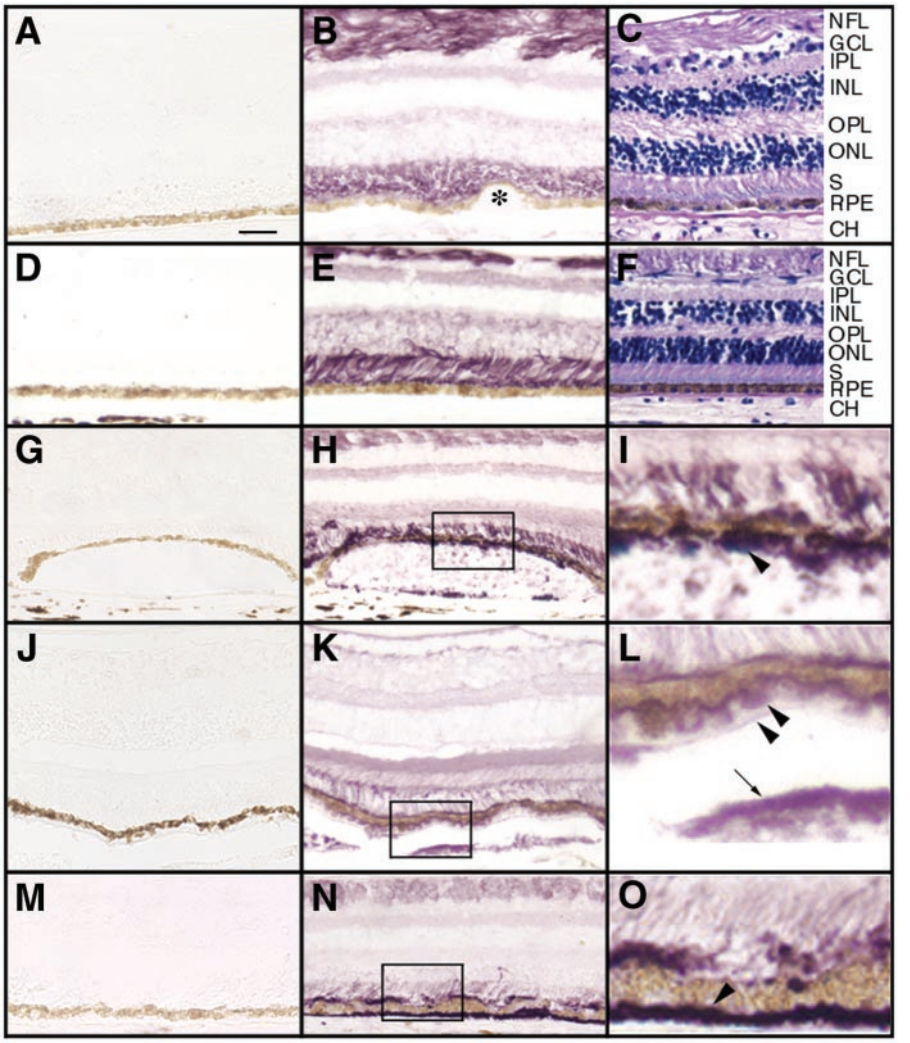

Fig. 4. The distribution of EFEMP1 in normal or AMD eyes. Paraffin sections were probed with Mab3-5 (*B*, *E*, *H*, *I*, *K*, *L*, *N*, and *O*) or the control mouse monoclonal antibody RET-PE2 (*A*, *D*, *G*, *J*, and *M*). Vector VIP (purple color) was used as substrate, and nuclei were not counterstained. Some sections were stained by hematoxylin/eosin (*C* and *F*) to illustrate the morphology. (*A–C*) Normal eye from a 91-yr-old female. Again, note that EFEMP1 staining is predominantly associated with the nerve fiber layer (NFL) and the photoreceptor inner and outer segments (S). No staining was observed in the RPE, Bruch's membrane, the choroid (CH), or small hard drusen (*B*, asterisk). (*D–F*) The peripheral region of the AMD eyes where no pathology was observed. Note the EFEMP1 staining (*E*) is similar to that in normal eyes (*B*). (*G–I*) The macular region of an AMD eye. *I* is higher magnification of the box area in *H*. Note intense EFEMP1 staining beneath the RPE immediately overlaying a soft druse (*H* and *I*, arrowhead). (*J–L*) The macular region of a second AMD eye. *L* is higher magnification of the box area in *K*. Again, note the heavy EFEMP1 staining beneath the RPE overlaying soft drusen (*K* and *L*, arrowheads). In this eye, drusen were also stained by the EFEMP1 antibody (*K* and *L*, arrow), and there is EFEMP1 staining condensed along the apical surface of the RPE, leaving the photoreceptor inner and outer segment staining less intense. (*M–O*) The macular region of a third AMD eye. *O* is higher magnification of the boxed area in *N*. Note heavy EFEMP1 staining of basal deposits (*N* and *O*, arrowhead). There is also heavier EFEMP1 staining at the apical surface of the RPE and less intense staining in the photoreceptor inner and outer segment region. GCL, ganglion cell layer; IPL, inner plexform layer; INL, inner nuclear layer; OPL, outer plexform layer; ONL, outer nuclear layer. [Scale bar = 50 μm (*A–H*, *J*, *K*, *M*, and *N*) and 12.5 μm (*I*, *J*, and *O*).]

Discussion

Here, we have demonstrated that mutant EFEMP1 carrying the R345W mutation associated with ML is misfolded and secreted inefficiently. Importantly, our data provide a link between ML and AMD. In both ML and AMD eyes, abnormally accumulated EFEMP1 is associated with the retinal pathology; that is, accumulation is seen only beneath the RPE overlaying sub-RPE deposits. Our findings suggest that the R345W mutation associated with ML may accelerate the same process of drusen formation that occurs in AMD. This finding may explain why *EFEMP1* mutations have not been found in AMD patients. If an *EFEMP1* mutation were found, the pathogenic process would be faster, the onset of the disease earlier, and the resulting disease diagnosed as ML rather than AMD.

ML is an autosomal, dominantly inherited disease. Although at this point the function of EFEMP1 is unknown, our finding that the R345W mutation results in protein misfolding may explain the dominant mode of inheritance. During protein biosynthesis, misfolded proteins can associate with and inhibit the successful folding of newly synthesized normal polypeptides and result in protein aggregation (22). Mutant EFEMP1 could interfere with the folding of the wild-type allele and thereby disturb its function.

In the absence of a mutation, it is possible that modifications due to oxidative, thermal, or other stress cause denaturing alterations of EFEMP1, resulting in the accumulation of EFEMP1 in AMD eyes. For example, point mutations cause α-synuclein to accumulate in Lewy bodies in autosomal domi-

nant inherited Parkinson's disease, whereas oxidatively modified α-synuclein is found in Lewy bodies in nonfamilial cases of Parkinson's disease (23). Epidemiologic data support a role for oxidative damage in the etiology of AMD (24), and the high local oxygen tension and exposure to light result in a highly prooxidative environment in the retina. In some individuals, a reduced ability of the macula to cope with the highly reactive oxygen species could lead to oxidatively denatured EFEMP1 accumulation.

Our findings provide evidence linking abnormal protein accumulation resulting from defects in protein folding, degradation, or transport to the pathology of AMD. Intracellular and extracellular deposition of defective protein aggregates is a characteristic feature of a wide variety of degenerative diseases, including the most common neurodegenerative diseases, Alzheimer's disease and Parkinson's disease (22). Protein aggregates can directly impair the ubiquitin proteasome system (25), and trigger apoptosis (26). The inefficient secretion and accumulation of EFEMP1 in RPE cells could lead to EFEMP1 aggregation and in time cause cellular degeneration. Protein aggregates are also thought to act as physical barriers to transport and other essential cellular functions. The photoreceptors lack a direct blood supply and rely on the RPE for nutrient supply and waste removal. Abnormal accumulation of EFEMP1 between the RPE and Bruch's membrane, or within Bruch's membrane, may create a physical barrier to transport between the RPE and the choroidal blood supply, resulting in the additional accumulation of other molecules, thereby forming drusen and other sub-RPE deposits.

We thank J. B. Stanton for technical support and C. Duchala for assistance with antibody production. We also thank O. Bernasconi for his help in obtaining the ML donor eye. Other human donor eyes were obtained from the Lions Eye Bank of Oregon and the Cleveland Eye Bank. We are grateful to P. Ousley and R. Dunway of the Lions Eye Bank of Oregon for their assistance. This work was funded by National Institutes of Health Grants EY13847 (to L.Y.M.) and EY13160 (to A.D.M.), a Kirchgessner Foundation grant (to A.D.M.), and Swiss National Science Foundation Grant 32-065250.01 (to F.L.M.).

1. Doyne, R. W. (1899) *Trans. Ophthalmol. Soc. U.K.* **19,** 71.
2. Vogt, A. (1925) in *Untersuchungsmethoden*, eds. Graefe, A. & Saemisch, T. (Verlag von Wilhelm Engelman, Berlin), 3rd Ed., pp. 1–118.
3. Klainguti, R. (1932) *Klin. Monatsbl. Augenheikd.* **89,** 253–254.
4. Evans, K., Gregory, C. Y., Wijesuriya, S. D., Kermani, S., Jay, M. R., Plant, C. & Bird, A. C. (1997) *Arch. Ophthalmol.* **115,** 904–910.
5. Collins, T. (1913) *Ophthalmoscope* **11,** 537–538.
6. Piguet, B., Haimovici, R. & Bird, A. C. (1995) *Eye* **9,** 34–41.
7. Fine, S. L., Berger, J. W., Maguire, M. G. & Ho, A. C. (2000) *N. Engl. J. Med.* **342,** 483–492.
8. Bressler, N. M., Bressler, S. B. & Fine, S. L. (1988) *Surv. Ophthalmol.* **32,** 375–413.
9. Klein, R., Klein, B. E. & Linton, K. L. (1992) *Ophthalmology* **99,** 933–943.
10. Vingerling, J. R., Dielemans, I., Hofman, A., Grobbee, D. E., Hijmering, M., Kramer, C. F. & de Jong, P. T. (1995) *Ophthalmology* **102,** 205–210.
11. Stone, E. M., Lotery, A. J., Munier, F. L., Heon, E., Piguet, B., Guymer, R. H., Vandenburgh, K., Cousin, P., Nishimura, D., Swiderski, R. E., *et al*. (1999) *Nat. Genet.* **22,** 199–202.
12. Lecka-Czernik, B., Lumpkin, C. K., Jr., & Goldstein, S. (1995) *Mol. Cell. Biol.* **15,** 120–128.
13. Ikegawa, S., Toda, T., Okui, K. & Nakamura, Y. (1996) *Genomics* **35,** 590–592.
14. Giltay, R., Timpl, R. & Kostka, G. (1999) *Matrix Biol.* **18,** 469–480.
15. Ozaki, T., Kondo, K., Nakamura, Y., Ichimiya, S., Nakagawara, A. & Sakiyama, S. (1997) *Biochem. Biophys. Res. Commun.* **237,** 245–250.
16. Marmorstein, L. Y., Ouchi, T. & Aaronson, S. A. (1998) *Proc. Natl. Acad. Sci. USA* **95,** 13869–13874.
17. Marmorstein, L. Y., Kinev, A. V., Chan, G. K., Bochar, D. A., Beniya, H., Epstein, J. A., Yen, T. J. & Shiekhattar, R. (2001) *Cell* **104,** 247–257.
18. Marmorstein, A. D., Csaky, K. G., Baffi, J., Lam, L., Rahaal, F. & Rodriguez-Boulan, E. (2000) *Proc. Natl. Acad. Sci. USA* **97,** 3248–3253.
19. Marmorstein, A. D., Marmorstein, L. Y., Rayborn, M., Wang, X., Hollyfield, J. G. & Petrukhin, K. (2000) *Proc. Natl. Acad. Sci. USA* **97,** 12758–12763.
20. Freedman, R. B. (1989) *Cell* **57,** 1069–1072.
21. Gerber, D., Munier, F. L. & Niemeyer, G. (2002) *Invest. Ophthalmol. Visual Sci.*, in press.
22. Sherman, M. Y. & Goldberg, A. L. (2001) *Neuron* **29,** 15–32.
23. Giasson, B. I., Duda, J. E., Murray, I. V., Chen, Q., Souza, J. M., Hurtig, H. I., Ischiropoulos, H., Trojanowski, J. Q. & Lee, V. M. (2000) *Science* **290,** 985–989.
24. Evans, J. R. (2001) *Prog. Retinal Eye Res.* **20,** 227–253.
25. Bence, N. F., Sampat, R. M. & Kopito, R. R. (2001) *Science* **292,** 1552–1555.
26. Gabai, V. L., Meriin, A. B., Yaglom, J. A., Volloch, V. Z. & Sherman, M. Y. (1998) *FEBS Lett.* **438,** 1–4.